SKB

TECHNICAL REPORT

92-04

Low temperature creep of copper intended for nuclear waste containers

P J Henderson, J-O Österberg, B Ivarsson

Swedish Institute for Metals Research, Stockholm

March 1992

LOW TEMPERATURE CREEP OF COPPER INTENDED FOR NUCLEAR
WASTE CONTAINERS

P J Henderson, J-O Österberg, B Ivarsson

Swedish Institute for Metals Research, Stockholm

March 1992

LOW TEMPERATURE CREEP OF COPPER INTENDED FOR NUCLEAR WASTE CONTAINERS

P. J. Henderson, J.-O. Österberg and B. Ivarsson
Swedish Institute for Metals Research
Drottning Kristinas väg 48
114 28 Stockholm

Keywords: Copper, creep, cracking, cavity

ABSTRACT

Creep tests have been carried out on oxygen-free high purity copper (Cu-OF) oxygen-free phosphorus copper (Cu-OFP) and oxygen-free copper containing 0.15 wt% Ag (Cu-OFS) at temperatures between 180 and 450°C. Some Cu-OF batches exhibited poor ductility and ruptured at creep strains of less than 1% while another batch produced acceptable ductility values of about 10% elongation at fracture. These differences in ductility were attributed to a combination of sulphur content and grain size. Specimens of Cu-OFP and Cu-OFS ruptured at creep strains of 30% or greater. It was speculated that small additions of P or Ag could increase the solid solution of S in copper and therefore reduce the risk of grain boundary segregation and embrittlement or that an element like P co-segregates with S and competes for grain boundary sites.

1.   INTRODUCTION

A method of nuclear waste disposal has been proposed whereby nuclear fuel is placed in cylindrical canisters of OF copper and lead is cast on top of it. The canisters are then sealed with top end pieces of copper, which are electron-beam welded into place. The canisters are to be located in granitic rock with bentonite clay around them. The heat from the fuel elements will give rise to temperatures of up to 100°C for a period of many thousands of years. At the same time ground water will gradually be absorbed in the bentonite giving rise to an external pressure of up to 15 MPa.

These conditions will cause creep deformation of the canisters. The total deformation will be small since it is limited by the inevitable casting porosity (2%) in the lead. When the lead has been sufficiently compressed so that the porosity has been removed, a hydrostatic pressure will be built up on the inside, which is identical to that on the outside and no further deformation will occur. This corresponds to a maximum local deformation of less than 5%. This is however, sufficient to be considered in detail in the design of the canisters. Even more important is the fact that local deformation can occur at the welded joints, which may have inferior creep properties to the parent material. Even small creep rupture cracks on the outside must be avoided. Although the corrosion properties of pure copper are excellent, the presence of cracks can initiate stress corrosion cracking. The design of the canisters is made on the explicit assumption that cracks should not be present.

Results of an earlier creep test series on parent metal showed that high elongation to fracture (30-40%) could be achieved at high stresses and low temperatures ($\leq$ 100°C), but at temperatures above 145°C and stresses below 100 MPa the elongation was less than 10% (1, 2).

Further tests on OF copper at higher temperatures and lower stresses (reported here) revealed a large reduction in ductility and necessitated a change of alloy to include small additions of phosphorus and silver.

2. EXPERIMENTAL

2.1. Mechanical Testing

Creep tests were preformed in air in unaxial tension on cylindrical specimens with a 5 mm diameter and 50 mm gauge length. Deformation was measured by extensometers attached to ridges on adaptors on either end of the specimen. It was assumed that no deformation took place outside the specimen gauge length or in the adaptors. Temperature was monitored by two thermocouples attached to the specimen gauge length.

2.2. Material

5 types of copper have been tested the chemical compositions of which are given in Table 1.

a) Creep series 000, Cu-OF. Specimens 31-53. Grain size = 60 μm. Same material as reported in IM-2384. 100 x 100 mm forged bars.

b) Creep series 100, Cu-OF. Specimens 101-105. Grain size = 370 μm. Material taken from the edge of two 100 x 100 mm forged bars, which had been electron beam welded together longitudinally.

c) Creep series 200, Cu-OF. Specimens 201 - etc.. Grain size = 45 μm. 10 mm diameter hot extruded (800°C) bars.

d) Creep series 300, Cu-OFS, Cu 0.15 Ag. Specimens 301- etc. Grain size = 35 μm. 10 mm dia extruded bars.

e) Creep series 400, Cu - OFP. Specimens 401- etc. Grain size = 45 μm. 10 mm dia extruded bars.

2. 3. Metallography

Samples for metallography were sectioned then ground and polished to 1 μm in the usual manner using SiC paper and diamond paste. They were given a final polish in a paste of MgO made with boiled distilled water (to remove CO_2) with some glycerol and a few drops of ammonia. This final polish prevents smearing of the surface layers so helping to expose cracks and cavities. Some samples were etched in a solution containing 100 ml water, 10 g ammonium persulphate and a few drops of NH_3.

2. 4. Auger Analysis

Scanning Auger Microscopy was carried out on crept specimens by Michael Wiggins of Daltek AB. The samples were fractured at room temperature in the Auger Microprobe at a pressure less than 5×10^{-10} torr and the analysis was also carried out at this pressure. The beam current was 100 nA and voltage 10 kV.

3. RESULTS

3.1. Mechanical Testing

The results of the creep tests are presented in Table 2 and figures 1 to 5. In Fig 1 the results of all the 000 creep series (including those reported earlier in IM-2384) are plotted together with some results of oxygen-free, high purity copper tested by Vitovec at 425°C, (3). The figure shows minimum creep rate per hour versus applied stresses for various temperatures ranging from 75 to 250°C. At lower stresses and higher temperatures the gradient, n, of the lines is equal to ~4 and corresponds to a creep strain at failure of less than 10% (in the case of specimens 31-53, very much less than 10%). A slope of n ≃ 4 is produced by so-called "power-law creep" in a single phase material and is described by the Bailey-Norton equation:

$$\dot{\varepsilon} = A\sigma^n \exp\left(\frac{-Q}{RT}\right) \tag{1}$$

where $\dot{\varepsilon}$ is the creep rate, σ the applied stress, Q the activation energy, R the gas constant, T the absolute temperature and A is a constant.

Power-law break down gives n values much greater than 4, namely n = 27 at 75°C, 13 at 110°C and 10 at 145°C elongations of 15 to 35 % and transgranular fracture.

Steady-state creep rates per second versus stress for the 100 and 200 series are shown in Fig. 2. Some results of the 000 series (also shown in Fig. 1) and previously published data from the literature are included for comparison. The strains to failure for the latter fell in the range 5-10%.

Fig. 3 shows the failure strain (elongation) as a function of lifetime for the 000, 200 and 400 series. For pure copper at low temperatures and short times (high stresses) the elongation is high but falls progressively with increasing temperature and increasing lifetime (decreasing stress). For Cu-OFP the failure strain remains high. The secondary creep rate as a function of stress for Cu-OFP is shown in Fig. 4. For temperatures where there is more than one result, the slope n is about 10.

Larson-Miller plots for Cu-OF and Cu-OFP are given in Fig. 5. The Larson-Miller parameter, P_{LM}, was obtained by the following equation

$$P_{LM} = T(20 + \log t) \tag{2}$$

where T is the temperature in Kelvins and t is the time to rupture in hours. P_{LM} values for 000 series at 75 to 145°C were calculated from rupture data found in Ref. 1. It can be seen from Fig. 5 that these P_{LM} values fall on a common curve, but an increase in temperature

from 145 to 250°C progressively shifts the curves to higher P_{LM} values. The data for the 100 and 200 series of Cu-OF copper are also shown. There is much scatter in the Cu-OF values, which is mainly due to large differences in rupture ductilities. The P_{LM} values for Cu-OFP, which encompass 215 to 450°C fall on a common curve.

3. 2. Metallography

Cu-OF

All the Cu-OF copper samples (000 - 200) exhibited cracking and cavities at the grain boundaries (see Figs. 6 to 11). The difference between the samples depended on the amount of cracking and the amount of deformation of the grains. Specimens tested at low temperatures (1) exhibited more deformation within the grains and very few cavities. However, cavities were visible in specimens tested at temperatures as low as 75°C (Fig 6) although the failure strain was high (17%). Specimen 104 showed very few cracks near the fracture and no cracks away from the fracture (Fig. 8 a), but 101 contained fine cracks and cavities along the full gauge length. The cavities appeared to have nucleated on small inclusions (Fig. 8 b). Chemical analysis in an ARL Scanning Electron Microscope Quantometer showed that these inclusions were enriched with sulphur. The fracture surfaces were highly cavitated (Fig. 9).Specimens 203 - 205 exhibited cracking along most of the gauge length (Fig. 10) and larger cavities and more localised ductility on the fracture surfaces (Fig. 11).

Cu-OFP

Specimens tested at 215°C showed highly deformed grains and a large amount of necking down at the fracture but no cracking or cavities, see Fig. 12 . At higher temperatures, eg 450°C, fracture occurred by growth and linkage of large, irregularly shaped cavities (Fig. 13). Cavities occurred along most of the gauge length and there was no evidence of deformation of the grains.

Cu-OFS

This alloy tested at 215°C showed highly elongated and deformed grains and also some small cracks and cavities (Fig. 14).

3. 3. Auger Analysis

Cu-OF 102 and 104.

The fracture surfaces obtained in the Auger Microprobe were cavitated (dia ~50 μm) and therefore similar to a creep fracture (Fig. 15). Mapping yielded an abundance of sulphur at the base of the cavities whilst the ridges contained only copper and no sulphur. The amount of sulphur on the fracture surface was estimated to be 8 at% although local areas as high as 13 at% were found.

Cu-OF 204

The fracture surface of this sample was more ductile, showing a larger cavity size of about 100 µm in diameter which again corresponds to a creep rupture surface of this material. Some sulphur was found on the surface, but it was not so evenly distributed as in the 100 series specimens. The surface sulphur content was estimated as 2 at%.

Cu-OFP

402 A ductile fracture surface was obtained and it was impossible to detect any sulphur.

411. The fracture surface contained large dimples, 200 µm in diameter which were enriched in sulphur, some areas containing as much as 14 at%. A sulphur rich particle was also located. It was not possible to detect phosphorus.

4. DISCUSSION

4. 1. Effect of grain size, temperature and strain rate.

The effect of grain size on creep crack growth has been investigated in a single phase austenitic stainless steel (9). The crack growth rate was found to increase with increasing grain size and the sensitivity of crack growth rate to the stress intensity factor also increased with increasing grain size. Grain boundary triple points were identified as the main barriers to crack propagation.

The influence of grain size on the creep ductility of copper is shown in Fig. 16, taken from Ref. 10. The strain rate used, 10^{-2} h^{-1}, is more than an order of magnitude greater than the highest creep rates recorded in the present investigation but Fig. 16 clearly shows that peak ductility is obtained with a grain size of 50 - 100 µm at temperatures of 425°C and below and ductility falls with a further increase in grain size at these temperatures.

The effect of strain rate and temperature is shown in Fig. 17 (also taken from Ref. 10) and Fig. 18 (Ref. 11). A decreasing strain rate (increasing rupture life) decreases the ductility at a constant temperature. An increase in temperature up to 400 or 500°C also causes a drop in ductility. The same trends are displayed in Figure 3.

The creep test conditions for series 000, 100 and 200 are plotted on a deformation mechanism map (Fig. 19) and a fracture mechanism map (Fig. 20) taken from Refs 12 and 13 respectively. The circles represent the conditions under which faliure strain was greater than 10-11% and the crosses the conditions under which the strain was10-11% or less and intergranular. Fig. 19 shows that the calculated map is in good agreement with reality and Fig. 20 agrees well except at temperatures below 200°C.

4. 2 Effect of Sulphur

The solubility of sulphur in copper is given in Ref. 7 and is reproduced below.

Temperature	In 99.999% Cu		In Cu-OF (99.99%)	
(°C)	ppm S	at% S	ppm S	at% S
1000	70	0.0140	85	0.0170
900	26	0.0052	46	0.0092
800	9	0.0018	23	0.0046
700	3	0.0006	11	0.0022
600	1	0.0002	4	0.0008

The maximum solubility of sulphur in Cu-OF at 600°C is 4 ppm and below this temperature it will be less. The 000 and 100 creep series both contained 10 ppm S; therefore at the creep temperature there will be an excess of at least 6 ppm or 0.0012 at% S. The 200 material will have an excess of 2 ppm or 0.0004 at % S. If all this excess S segregates to grain boundaries there will be an average coverage of 0.36 atom layers in 000 material, 2.20 atom layers in 100 material and 0.09 atom layers in 200 materials. The amount of S present at the boundaries thus depends on a combination of S content and grain size.

The Auger analysis showed that S had segregated to the cavity surfaces at the grain boundaries. The driving force for this segregation is the reduction in surface free energy γ_s. According to classical nucleation theory, a cavity will become stable and grow when

$$r \geq 2 \gamma_s/\sigma \qquad (3)$$

where r is the cavity radius and σ the tensile stress. As an approximation, a strongly segregating species reduces the surface energy to 33-50% of its original "clean" value (14).

In the OF copper grain boundary sliding occurs (see for example Fig. 6 b) and stress concentrations arise at irregularities in the boundaries, such as triple points or at grain boundary particles. If this sliding is not accommodated by deformation within the grains (plasticity, creep or diffusion) then cracks or cavities will appear at the stress concentrations. Cavities can also form at the intersection of a slip plane with a grain boundary. Sulphur may affect the nucleation rate of cavities by forming sulphides like Cu_2S at grain boundaries which increases the number of nucleation sites. S also reduces the critical size for cavity growth via a reduction in the surface free energy.

4. 3. Effect of Phosphorus

A phase diagram for the Cu-P binary system (8) shows that the maximum solid solubility of P in Cu is 1.2 wt% (0.6 at%) at 300°C and about 0.6 wt% at 200°C which is significantly greater than the 50 ppm (0.005 wt%) P present. Most of this phosphorus will be in solution, but there will be some equilibrium segregation of phosphorus to the grain boundaries. With reference to the S solubility table it can be seen that a decrease in the purity of Cu increases the S solubility. It is possible that the addition of 50 ppm P or 1500 ppm Ag increases the S solubility and hence is an effective way of reducing the deleterious effects of S. Alternatively there could be some co-segregation of P and S and some competition for grain boundary sites. Auger spectroscopy of fracture surfaces of steels doped with S and P has shown that S and P are found on complementary areas of grain boundaries, (15). In addition, the deleterious effects of sulphur disappeared when small amounts of phosphorus were added to the steel, (15).

5. CONCLUSIONS

Oxygen-free high purity copper (Cu-OF) when tested at 180°C and above in the power-law creep regime exhibited strains to failure of about 10% or less, intergranular cracking and cavitation. In many cases the failure strains were less than 1% and this poor ductility was associated with a bulk sulphur content of 10 ppm and/or a large grain size. There is a strong possibility that the same poor ductility will be seen at lower temperatures and stresses, corresponding to service conditions.

Limited tests on oxygen-free phosphorus copper (Cu-OFP) and on oxygen-free silver copper (Cu-OFS) indicated that these two alloys do not suffer from the same ductility problems as Cu-OF and failure strains in the region of 30-50% were obtained. The improvement in ductility could be due to an increase in the S solid solubility or co-segregation of P or Ag and competition with S for grain boundary sites. Similar effects have been seen in steels.

In view of the difficulty in controlling the S content and maintaining a small grain size (<60 μm) over all areas of the nuclear waste canisters (including the welds) it is suggested that the Cu-OFP material be investigated further at lower creep temperatures and strain rates.

6. ACKNOWLEDGEMENTS

REFERENCES

1. IVARSSON, B and ÖSTERBERG, J-O
   "Creep Properties of Welded Joints in Cu-OF Copper for Nuclear Waste Containment".
   IM-2384, Aug. 1988.

2. IVARSSON, B., ÖSTERBERG, J-O , SANDSTRÖM, R. and WERME, L.
   "Creep Properties of Welded Joints in Copper Canisters for Nuclear Waste
   Containment". Mat. Res. Soc. Symp. Proc. 127, pp 397-402. Materials Research
   Society (1989).

3. VITOVEC, F. H. "Cavity Growth and Creep Rate taking into account the change of Net
   Stress". J. Mater. Sci. 7 (1972), 615-620.

4. JENKINS, W.D. and DIGGES, T. G."Creep of High Purity Copper". J. Res. of Nat.
   Bureau of Standards, 45, (1950), 153-173.

5. RAJ, S. V. and LANGDON, T. G. "Creep behaviour of copper at intermediate
   temperatures - 1. Mechanical Properties". Acta. Metall. 37, (1989), 843-852.

6. PARKER, J. D. and WILSHIRE , B. "Friction stress measurements during high
   temperture creep of polycrystalline copper". Metal. Sci. 12, (1978), 453- 458.

7. ELLIOTT, R. P. "Constitution of Binary Alloys - First Supplement" p. 381 Mc Graw -
   Hill (1965).

8. HANSEN, M. "Constitution of Binary Alloys" p. 608. Mc Graw-Hill, (1958).

9. ZHU, S. J., ZHU. S. M. and WANG, F. G. "Influence of grain size on the Creep Crack
   Growth Behaviour of Cr 15 Ni 25 Steel". Scripta Metall 23, (1989), pp 1845-1848.

10. FLECK, R. G., COCKS, G. J. and TAPLIN, M. D. R. "The Influence of Polycrystal
    grain size on the Creep Ductility of Copper". Met. Trans. 1,(1970), 3415-3420.

11. GREENWOOD, J. N., MILLER, D. R. and SUITER, J. W.
    "Intergranular Cavitation in Stressed Metals". Acta. Met. 2 (1954), 250-258.

12. FROST, H. J. and ASHBY, M. F., "Deformation - Mechanism maps", p 24, Pergamon
    Press, Oxford, (19892).

13. ASHBY, M. F. GANDHI, C. and TAPLIN, D. M. R., "Fracture - Mechanism Maps and their Construction for F.C.C. metals and alloys". Acta Metall. 27, (1979), 699-727.

14. HONDROS, E.D. and SEAH, M. P., "Segregation to interfaces", Int. Met. REv. 22, (1977), 262-301.

15. CHEN, S-H, TAKASUGI, T. and POPE, D. P., "The Effects of Trace Impurities on the Ductility of a Cr-Mo-V steel at elevated Temperatures". Met. Trans. 14 A, 571-580.

Table 1   Chemical Compositions of Test Material and Some Room Temperature Mechanical Property Data

Creep Series		000	100	200	300	400
		Cu-OF	Cu-OF	Cu-OF	Cu-OFS	Cu-OFP
Ag	g/t	-	-	-	1500	-
P	g/t	-	-	-	-	50
Ag	g/t	20	16	10	-	12
Al	g/t	1	1.5	<1	1	2
As	g/t	2	3	<1	<1	2
Bi	g/t	0.4	0.3	<1	<1	<1
Cd	g/t	<1	<1	<1	<1	<1
Co	g/t	<10	<10	<10	<10	<10
Cr	g/t	<3	<3	<3	<3	<3
Fe	g/t	6	5	2	2	7
H	g/t	0.16	0.69	<0.10	0.10	<0.10
Hg	g/t	<1	<1	<1	<1	<1
Mn	g/t	2	2	<1	<1	<1
Ni	g/t	3	3	<3	3	4
O	g/t	1.2	1.6	1.1	0.9	0.9
P	g/t	2	2	<1	<1	-
Pb	g/t	0.5	0.5	1	<1	<1
S	g/t	10	10	6	6	6
Sb	g/t	<3	3	<3	<3	4
Se	g/t	<1	<1	<1	<1	2
Si	g/t	<1	<1	<1	<1	<1
Sn	g/t	<3	<3	<3	<3	<3
Te	g/t	<3	<3	<3	<3	<3
Zn	g/t	9	<1	<1	<1	<1
Zr	g/t	<3	<3	<3	<3	<3
Grain size	(μm)	60	370	45	35	45
Yield strength	(MPa)			50	57	46
Tensile strength	(MPa)			234	246	239
Elongation	(%)			61	59	60
Hardness	(HV)			42	43	40

Table 2 Creep results.

Creep Series	Test mark	Temp (°C)	Stress (MPa)	t_f (h)	$\dot{\varepsilon}$-mcr (h^{-1})	$\dot{\varepsilon}$-mcr (s^{-1})	ε_f (%)	P_{LM} (10^3)
000	31	180	60	2247	1.44×10^{-6}	4×10^{-10}	0.9	10.58
Cu-OF	32	180	80	373	4.36×10^{-6}	1.2×10^{-9}	0.3	10.22
	33	180	100	102	1.64×10^{-5}	4.5×10^{-9}	0.3	9.97
	41	215	40	4623	5.4×10^{-7}	1.5×10^{-10}	0.8	11.55
	42	215	60	754	2.93×10^{-6}	8.1×10^{-10}	0.3	11.16
	43	215	80	86	1.71×10^{-5}	4.75×10^{-9}	0.25	10.70
->	51	250	20	16272	3.5×10^{-7}	9.7×10^{-11}	0.33	-->
	52	250	40	1660	2.05×10^{-6}	5.7×10^{-10}	0.7	12.14
	53	250	60	175	1.08×10^{-5}	3.0×10^{-9}	0.35	11.63
100	101	215	45	684	2.02×10^{-6}	5.61×10^{-10}	0.6	11.14
Cu-OF	102	215	55	250	?	?	0.15	10.93
	103	215	70	84	1.80×10^{-5}	5.03×10^{-9}	0.25	10.70
	104	215	85	33.5	2.60×10^{-5}	7.22×10^{-9}	0.30	10.50
*	105	215	36	3552	5.0×10^{-7}	1.39×10^{-10}	0.26	*
200 *	201	215	45	2016	2.16×10^{-6}	6.0×10^{-10}	0.69	*
Cu *	202	215	55	1368	8.28×10^{-6}	2.3×10^{-9}	1.38	*
OF	203	215	70	5058	1.44×10^{-5}	4.0×10^{-9}	12.2	11.57
	204	215	85	1030	6.1×10^{-5}	1.7×10^{-8}	11.1	11.23
	205	215	100	330	2.0×10^{-4}	5.5×10^{-8}	10.1	10.99
300 *	301	215	120	4920	?	?	2.7	*
Cu-	302	215	140	4618			27	11.55
OFS *	305	215	100	2400	?	?	1.0	*
	401	215	120	7848	4.5×10^{-5}	1.25×10^{-8}	35.5	11.66
400	402	215	140	1451	2.23×10^{-4}	6.2×10^{-8}	38.5	11.30
Cu ->	405	215	100	5520	4.6×10^{-6}	1.3×10^{-9}	3.2	-->
OFP	406	215	160	52	3.0×10^{-4}	8.49×10^{-8}	32.1	10.61
	407	215	150	192	1.19×10^{-3}	3.3×10^{-7}	40.7	10.87
	410	300	100	220	9.94×10^{-4}	2.8×10^{-7}	44.0	12.80
	411	450	30	195	8.9×10^{-4}	2.5×10^{-7}	32.1	16.11
	412	250	100	3047	1.45×10^{-5}	4.0×10^{-9}	41.6	12.38
	413	250	120	656	5.23×10^{-4}	1.45×10^{-7}	57.6	11.93

--> Test continuing

* Test interrupted
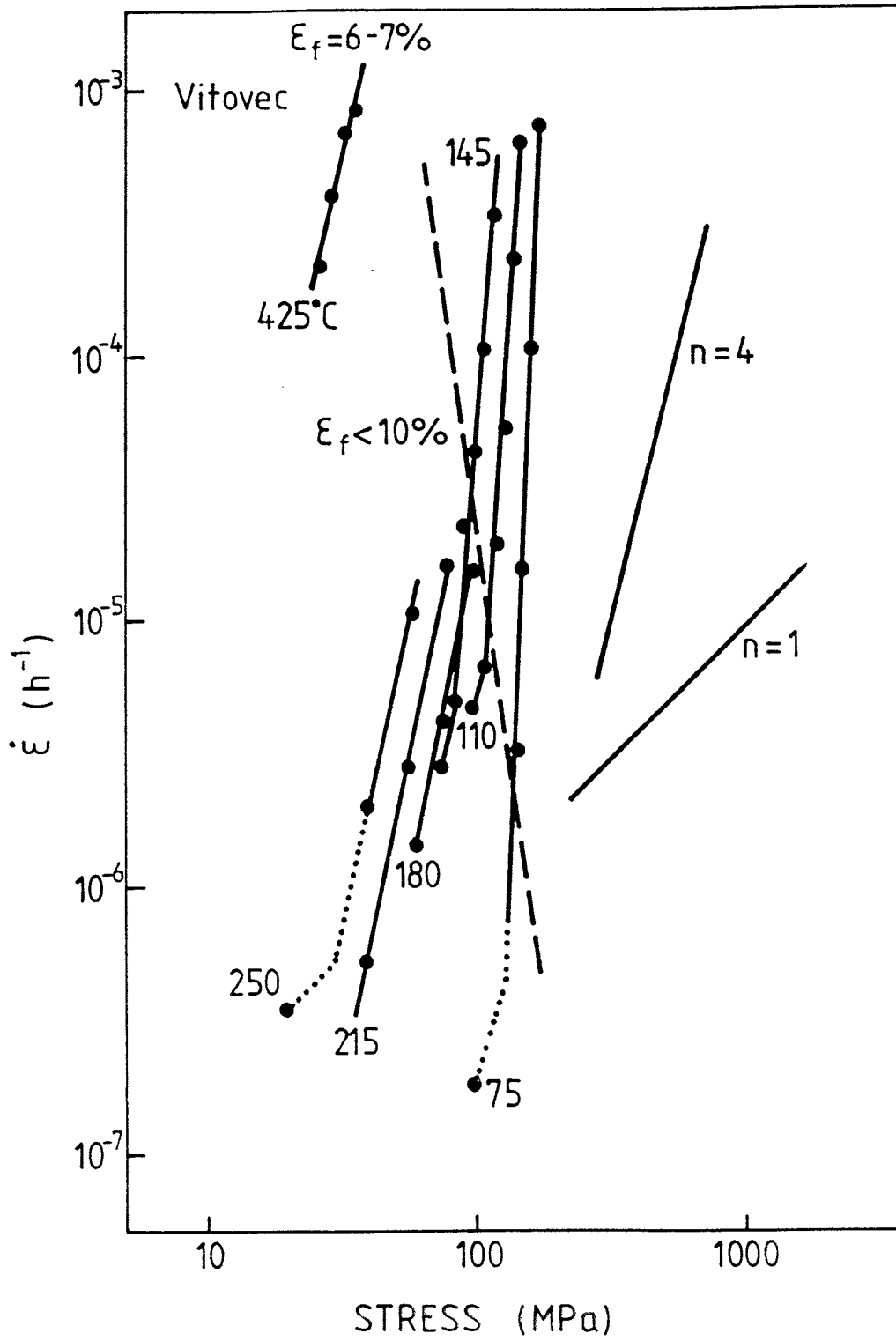
Fig 1. Plot of minimum state creep rate $\dot{\varepsilon}$ versus stress for 000 series Cu-OF. Data for 75-145°C have been taken from Ref. 1.
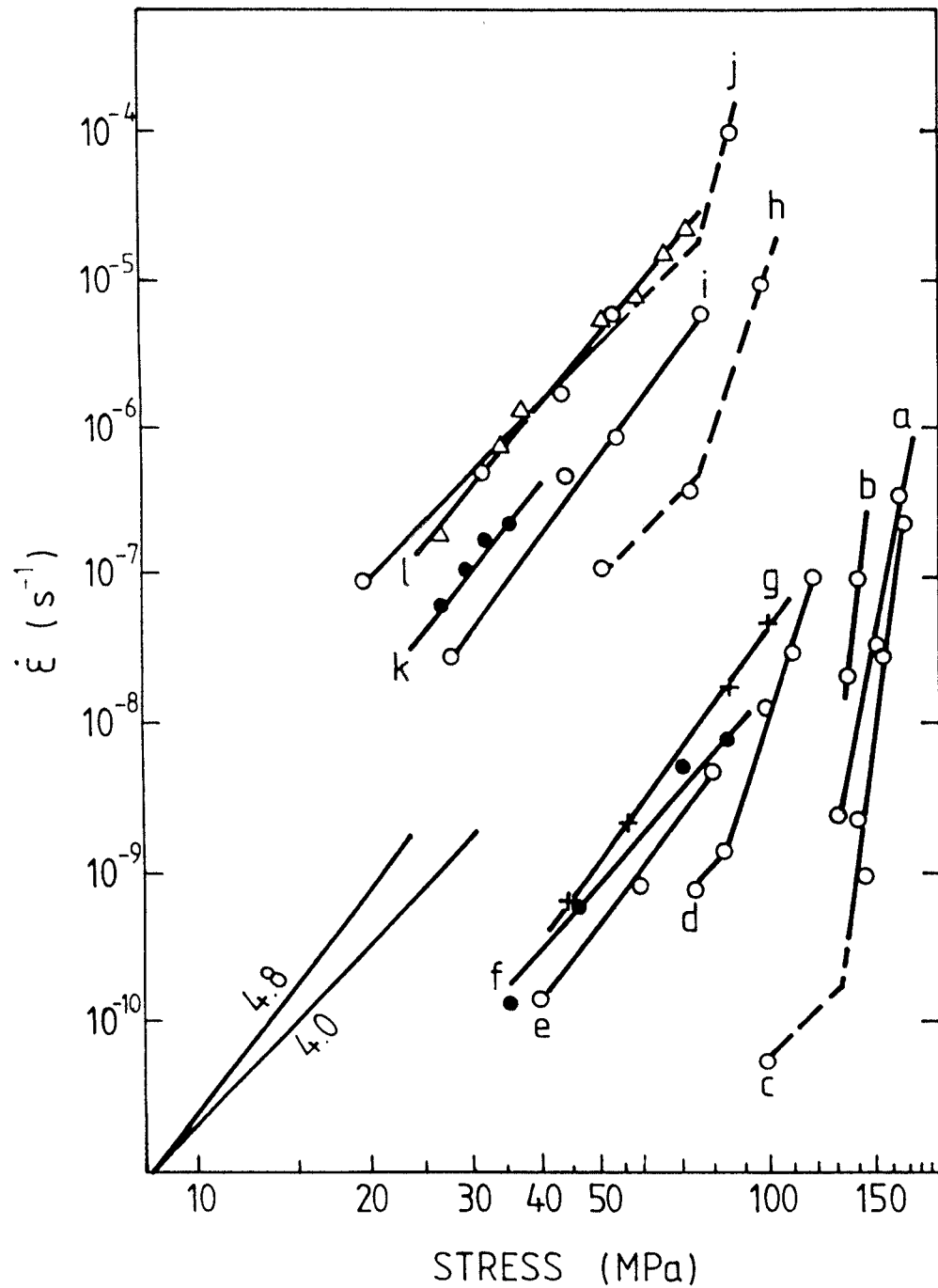
Fig. 2.

Minimum creep rate versus stress for Cu-OF copper.

(a) o Jenkins and Digges. Ref. 4 121°C. Grain size = 25 μm

(b) o Jenkins and Digges. Ref. 4 149°C. Grain size = 25 μm

(c) o Series 000 75°C. Grain size = 60 μm

(d) o Series 000 145°C.

(e) o Series 000 215°C.

(f) • Series 100 215°C. Grain size = 370 μm

(g) + Series 200 215°C. Grain size = 45 μm

(h) o Raj and Langdon. Ref 5. 350°C Grain size = 250 μm

(i) o Raj and Langdon. Ref 5. 400°C

(j) o Raj and Langdon. Ref 5. 450°C

(k) • Vitovec. Ref. 3. 450°C Grain size = 79 μm

(l) Δ Parker and Wilshire. Ref 6. 413°C Grain size = 200 μm
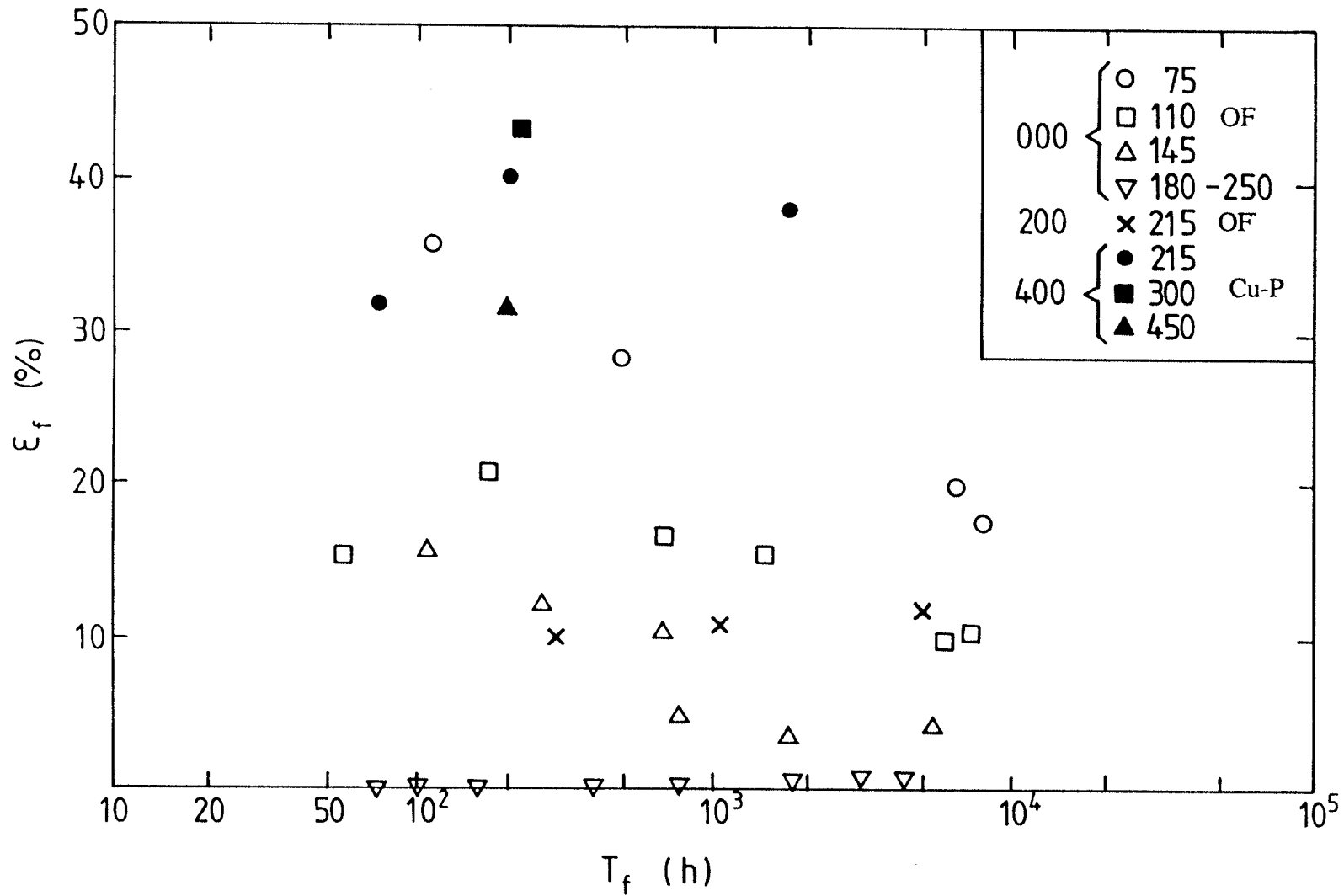
Fig. 3. Elongation at fracture, ε_f, as a function of time to fracture, t_f, for the Cu-OF series 000 and 200 and Cu-OFP 400 series at various temperatures given in °C. Data points for 100 specimens have not been plotted but coincide with the 180-250°C results of 000 specimens. Increasing temperature produced a dramatic reduction in ductility in the 000 material but did not affect the 400 specimens.
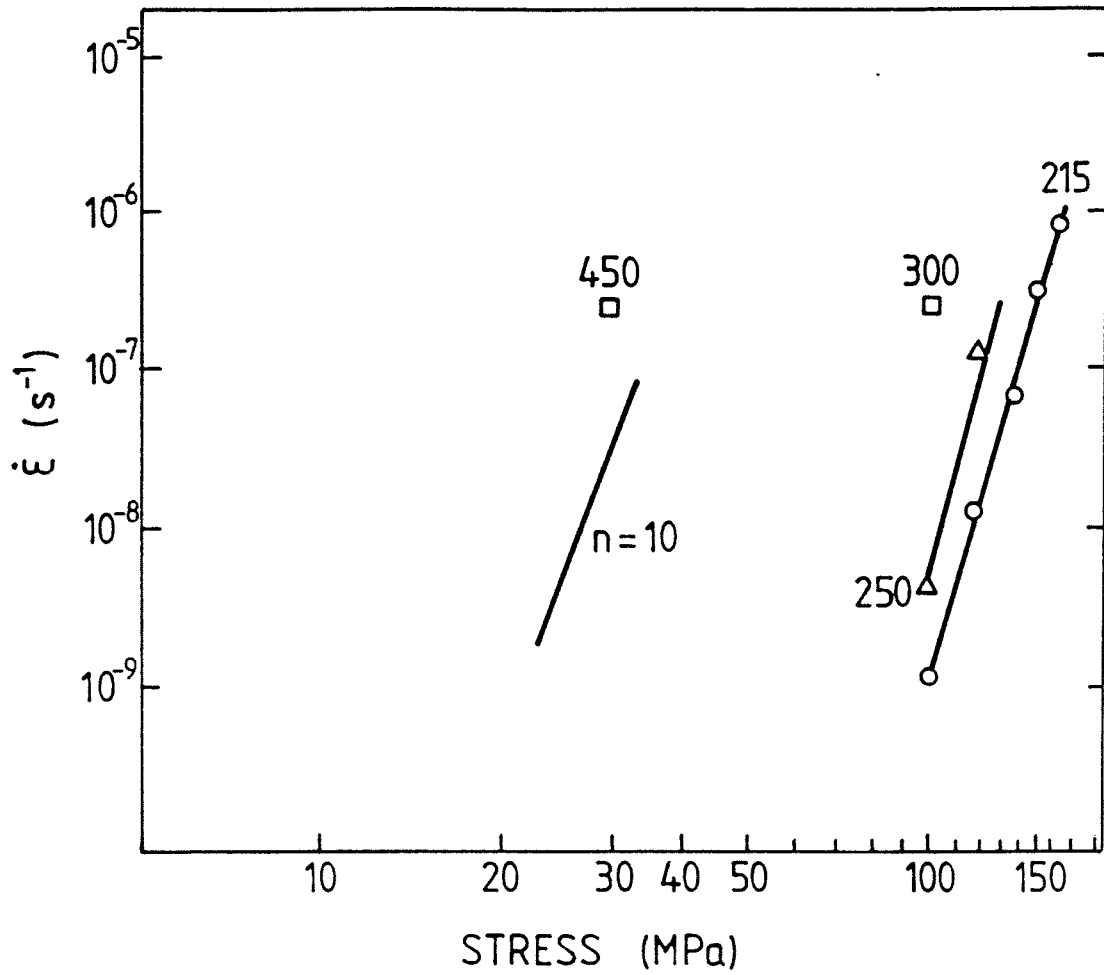
Fig. 4.   Creep rate as a function of stress for Cu-OFP material at various temperatures.
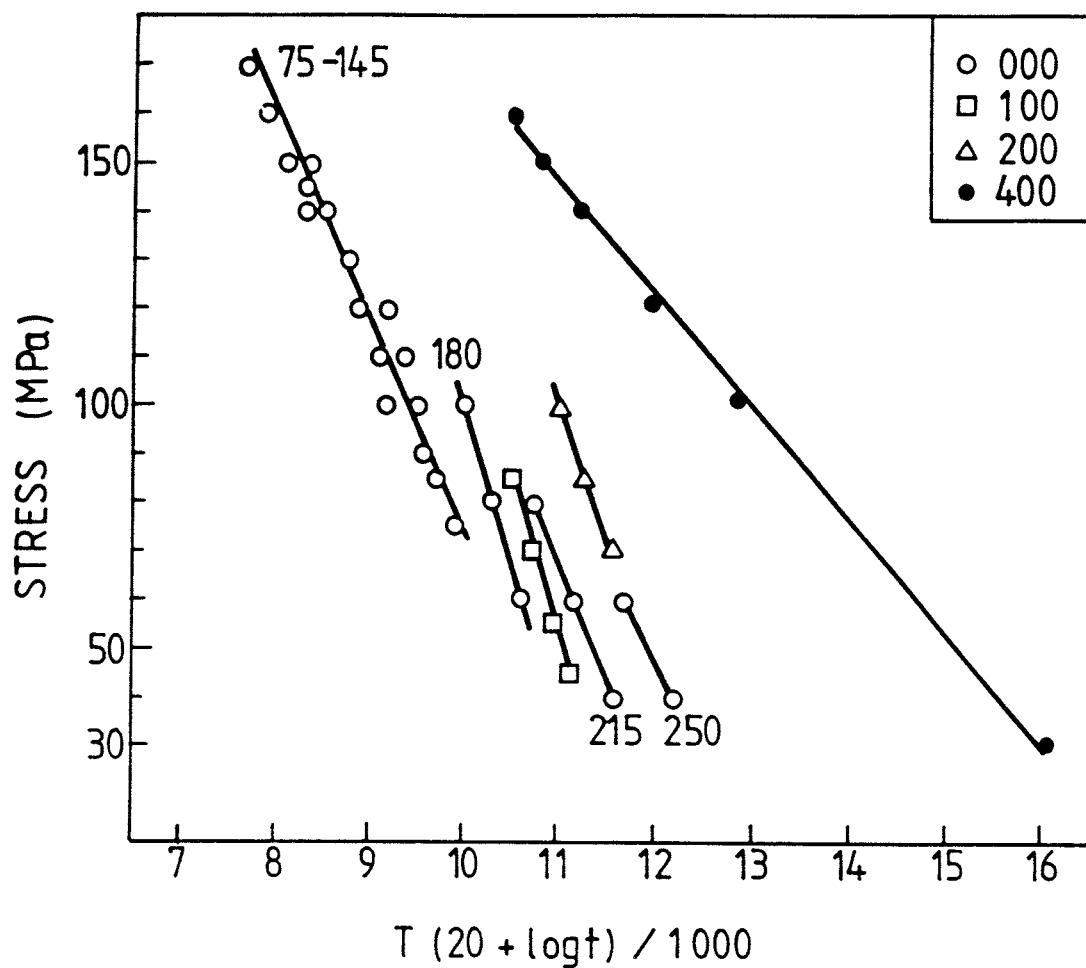
Fig. 5. Larson-Miller plot for all the Cu-OF specimens and Cu-OFP specimens. The figures near each curve refer to the test temperature in °C.
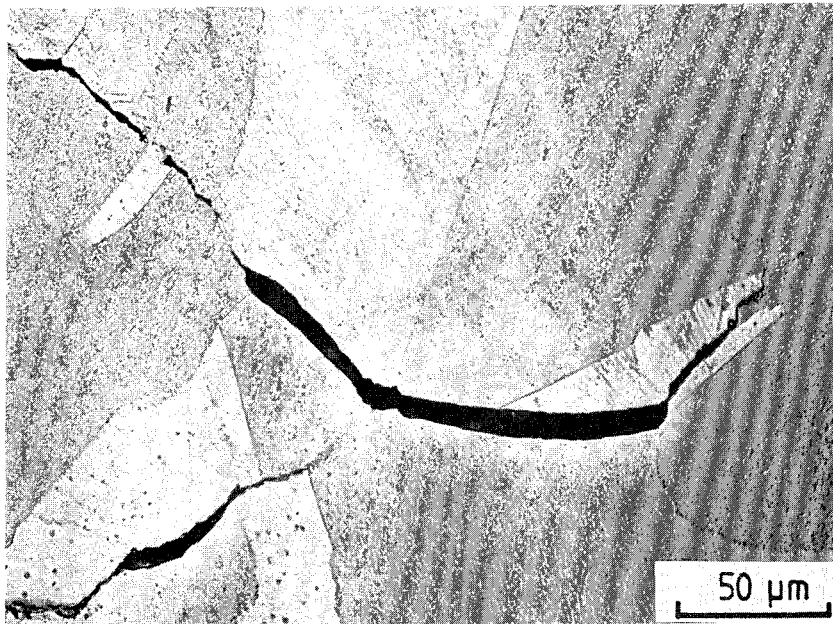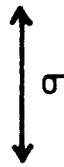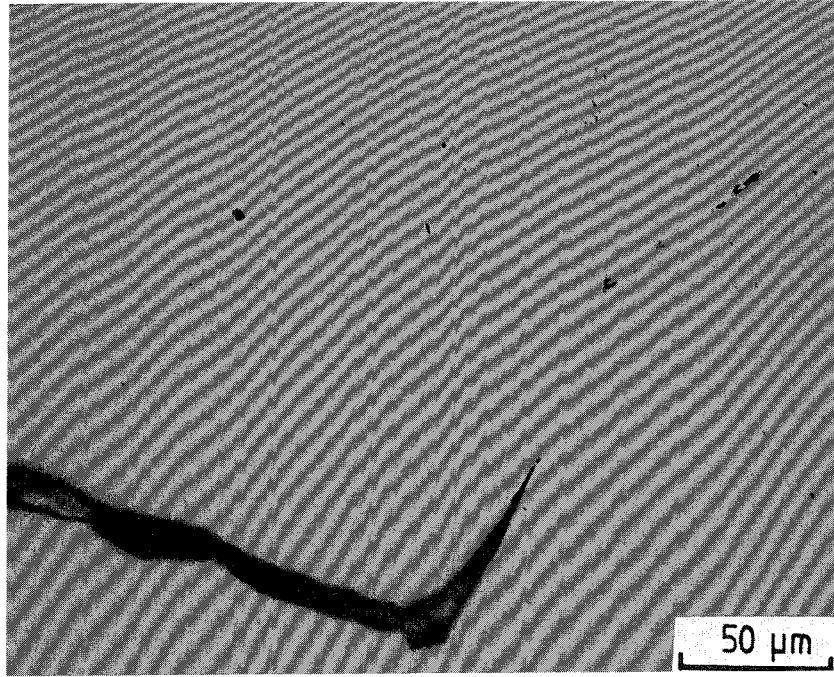
Fig. 6.   (a) Upper. Specimen 015. 75°C/ 140 MPa. ε_f = 20%. Partially polarised light,
unetched, showing cracking and small cavities.
(b) Lower Specimen 052. 250°C. Etched.
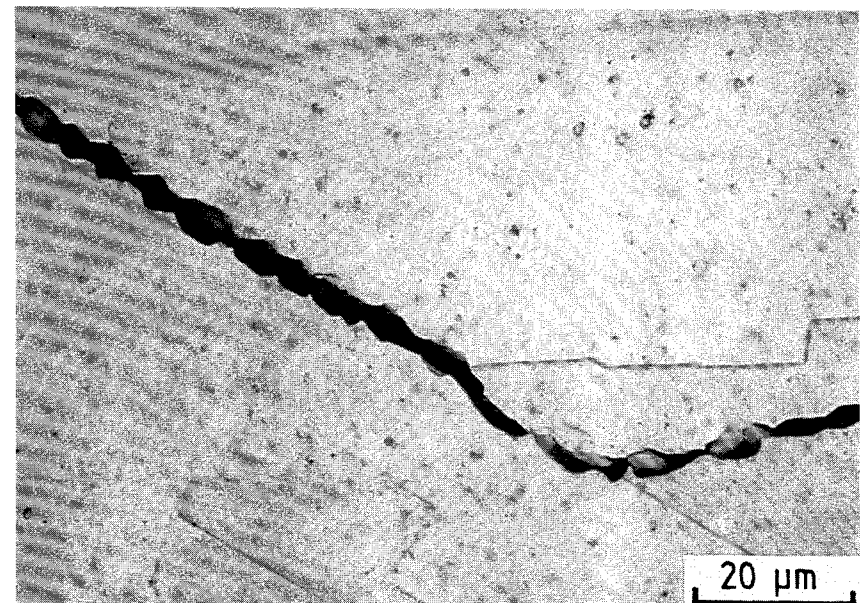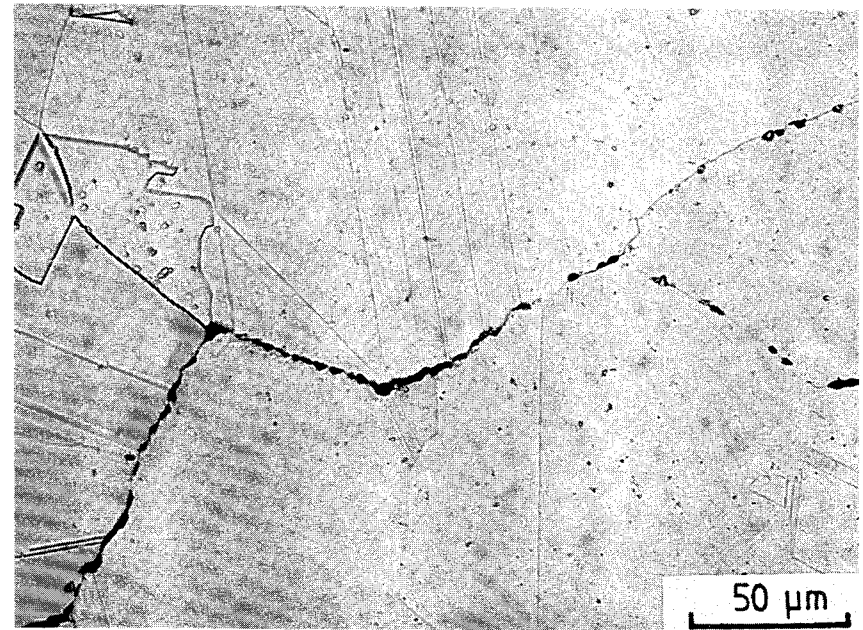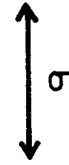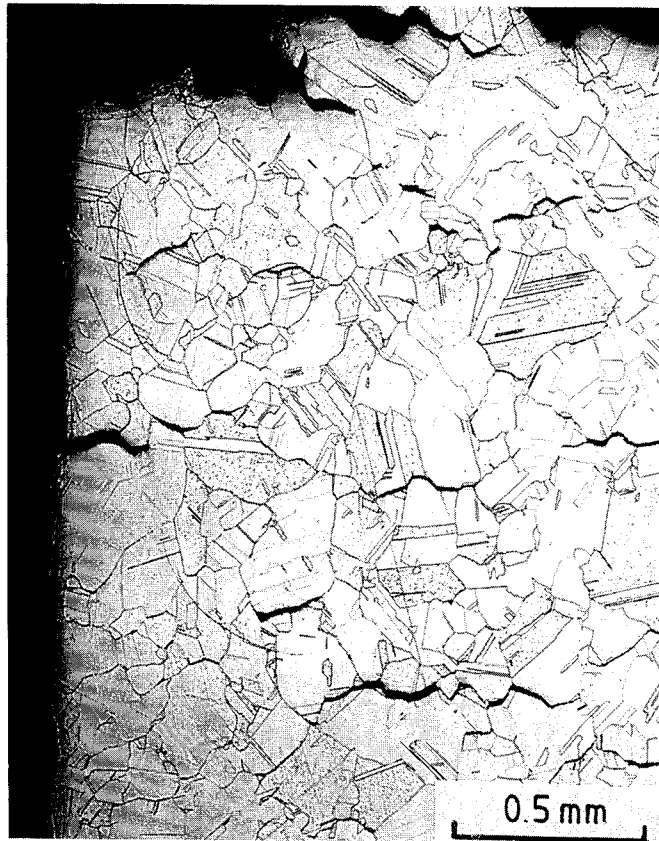
Fig. 7. Specimen 031 180°C/ 60 MPa $\varepsilon_f = 0.7\%$.
Grain boundary cracking seen at low
magnification, cavities at higher magnifications.

$\overset{\sigma}{\longleftrightarrow}$
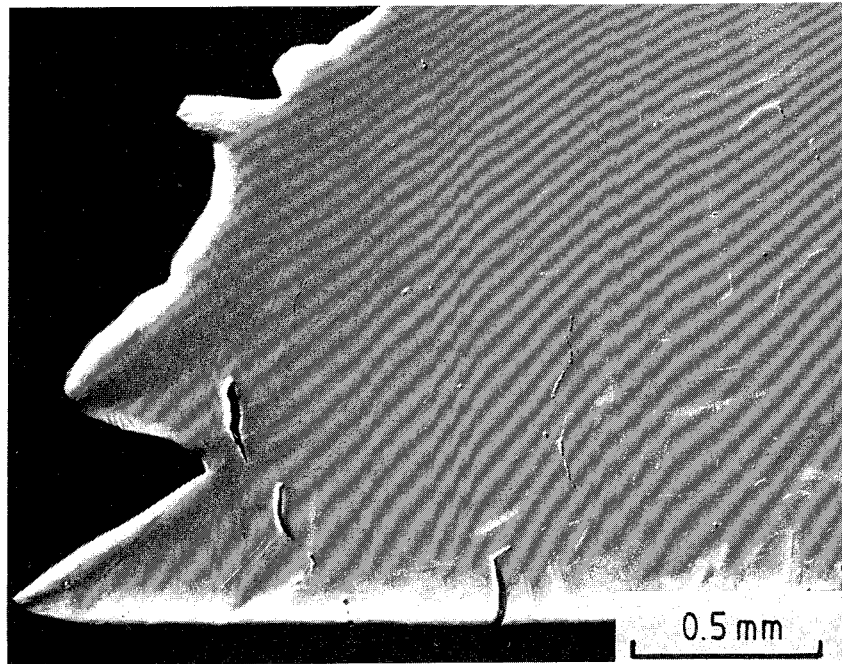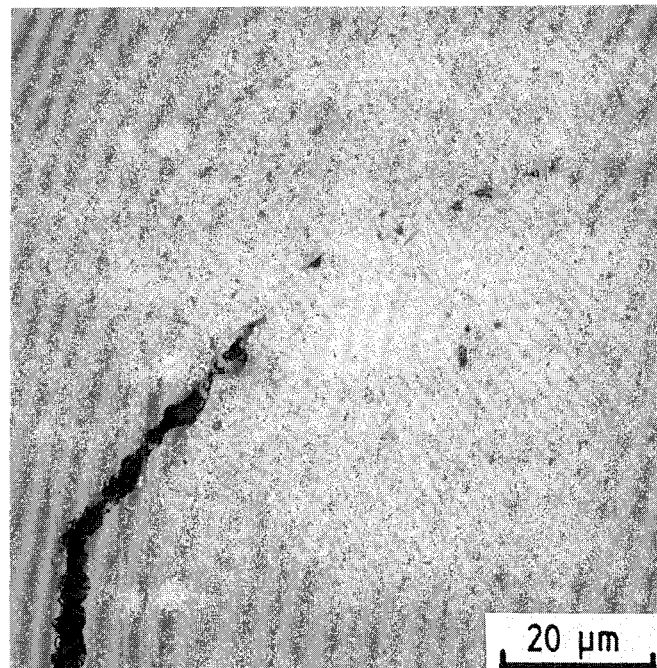
Fig. 8.   (a) Upper, Specimen 104. Unetched.

(b) Lower, Specimen 101. Unetched. Cracks and cavities along the gauge length but away from the fracture. The cavities appear to be nucleating on small inclusions.
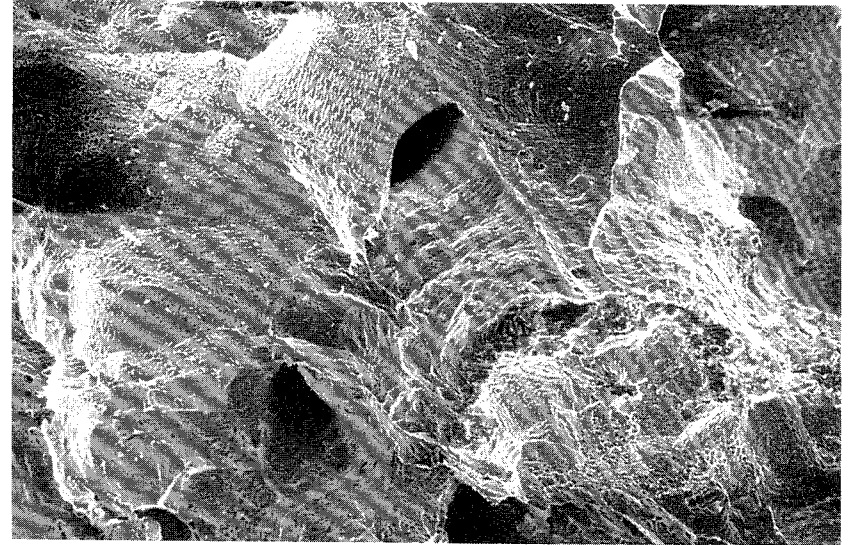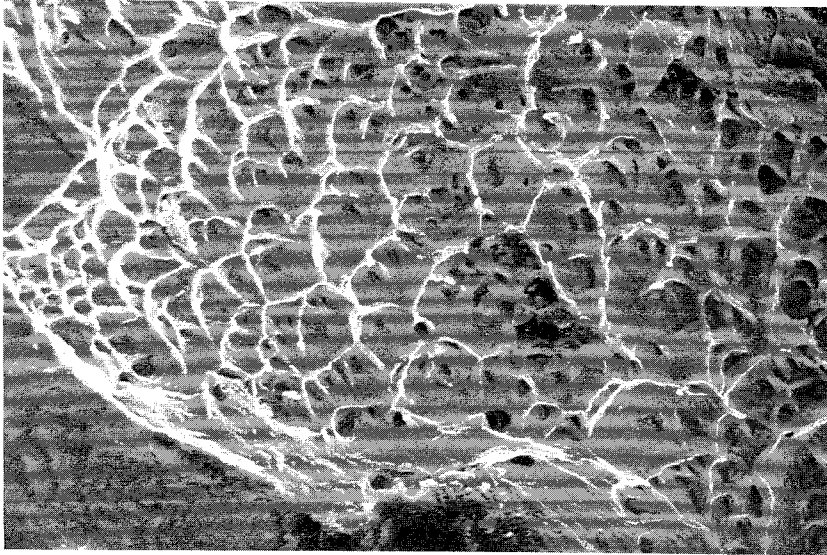
Fig. 9.   SEM micrographs of 104's fracture surface.
Grain boundary surfaces heavily cavitated.
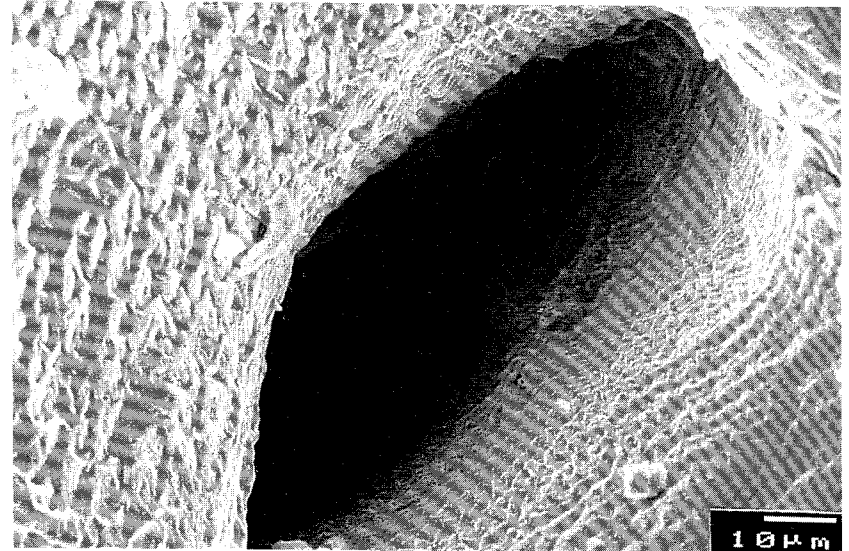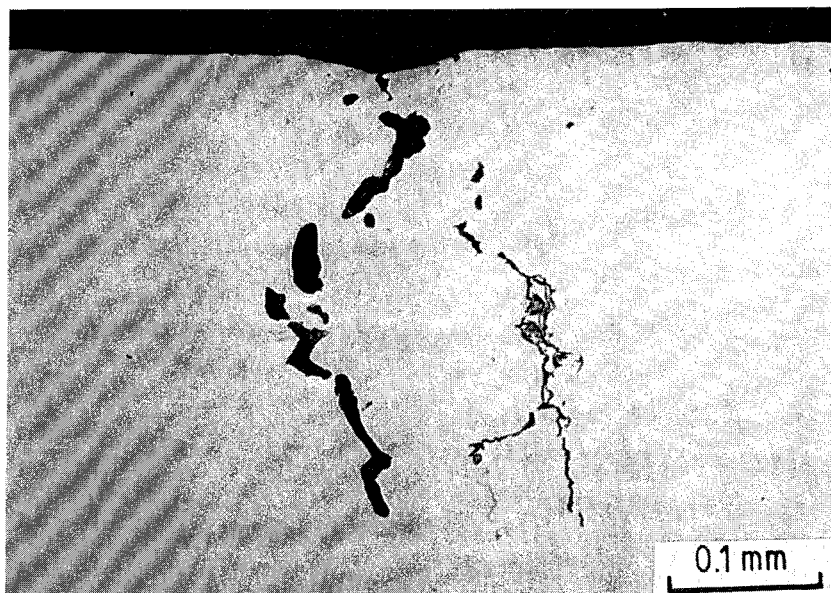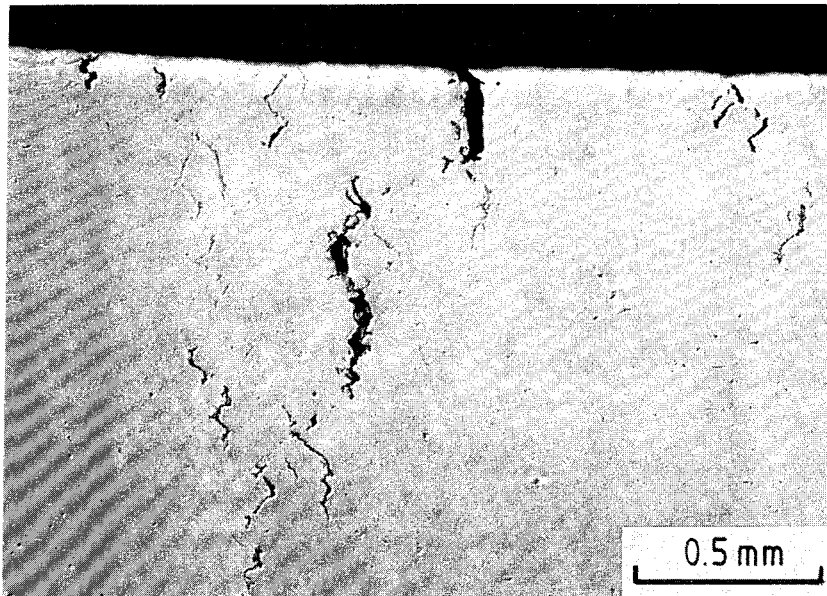
Fig. 10. Specimen 204, unetched

    (a) Upper. Near the fracture.

    (b). Lower. 7 mm from the fracture.
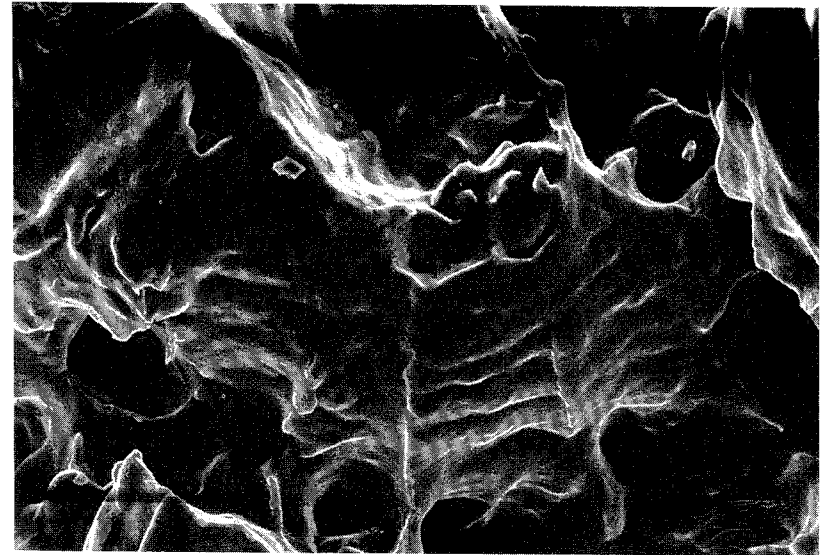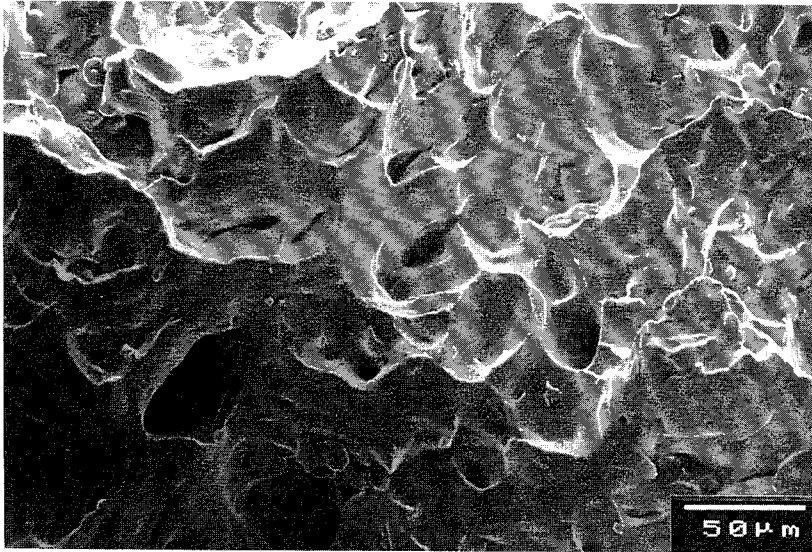
Fig. 11.

SEM micrographs of 204 and 205's fracture surfaces. Larger cavity size than in 104 (cf Fig. 9) and more evidence of ductility.

σ
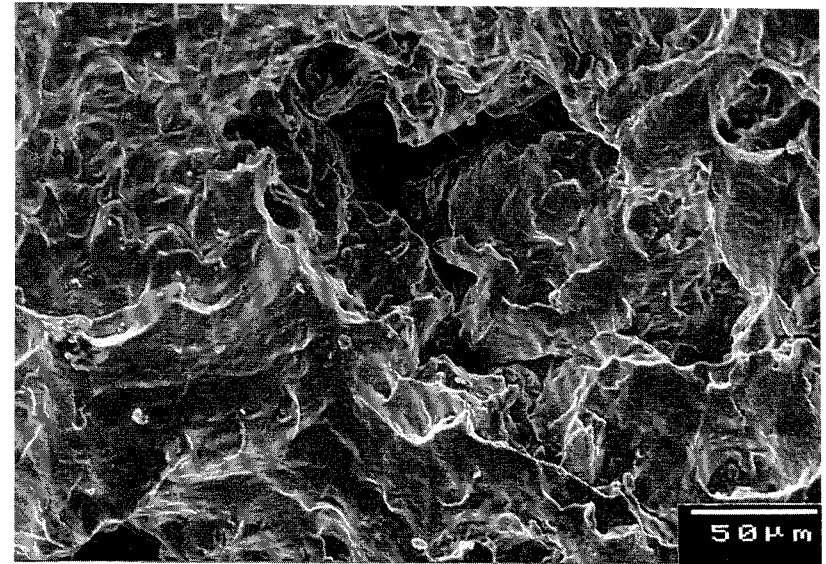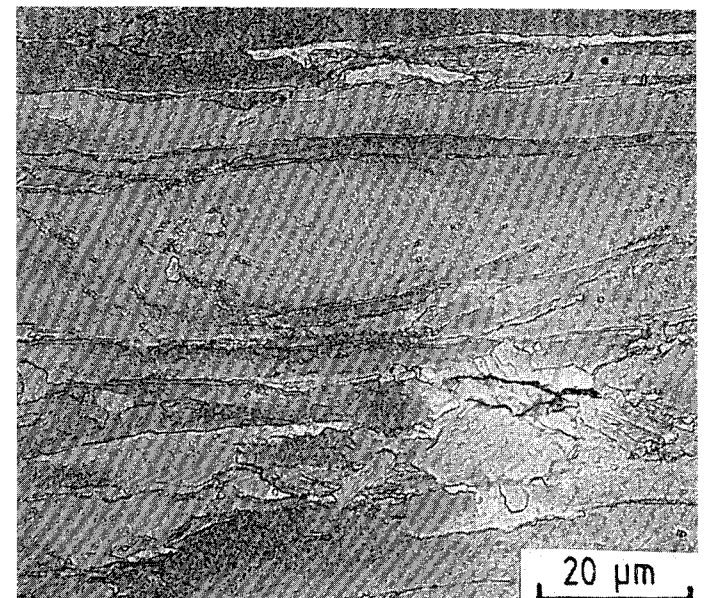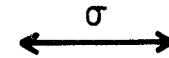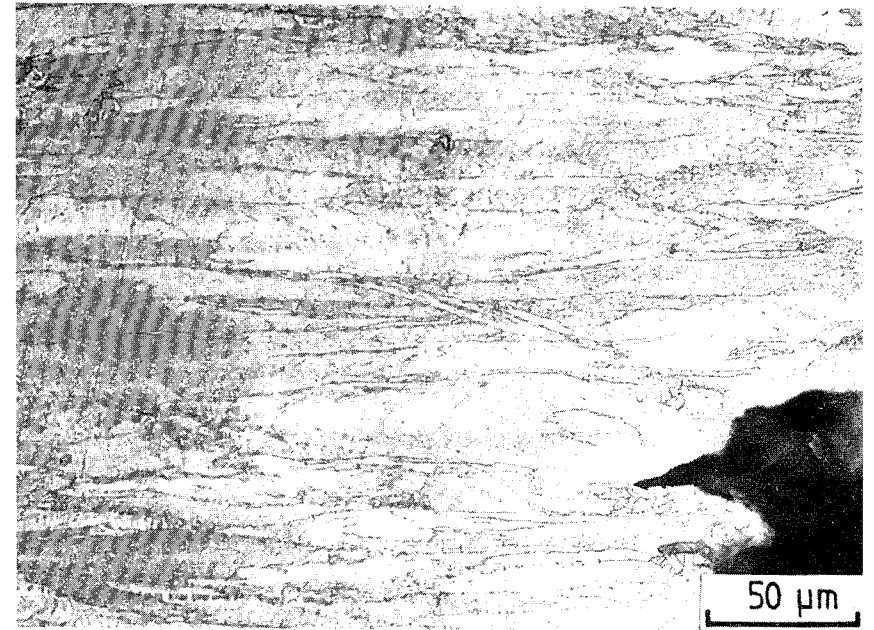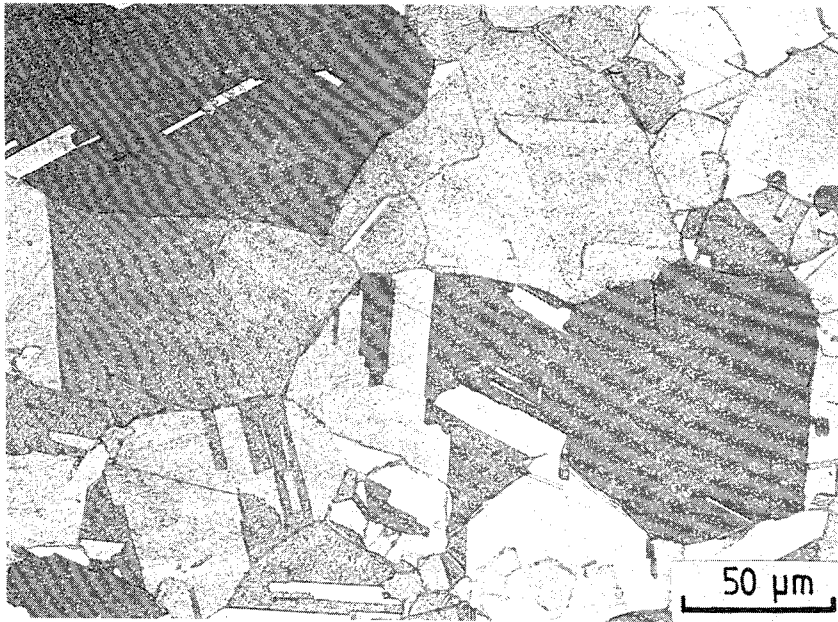
Fig. 12. Specimen 402, 215°C, Cu-OFP- Etched.

(a) above, undeformed grip end

(b) above right, at fracture, highly deformed grains.

(c) right, near fracture

σ
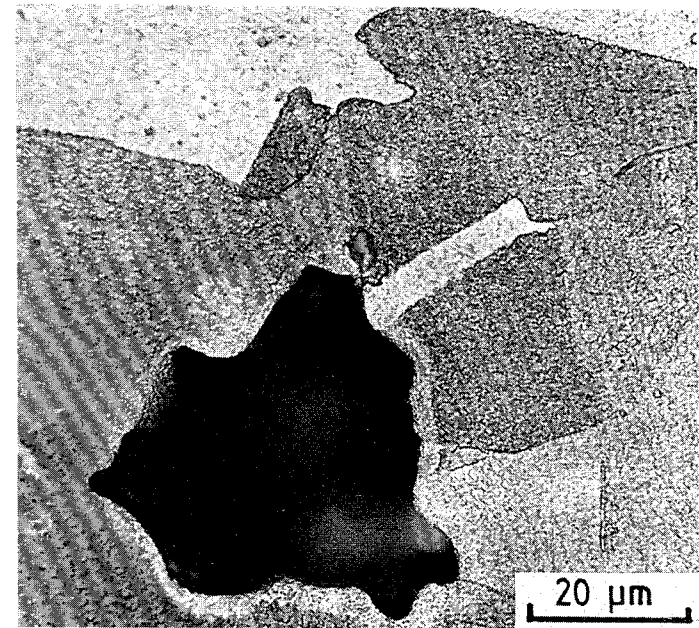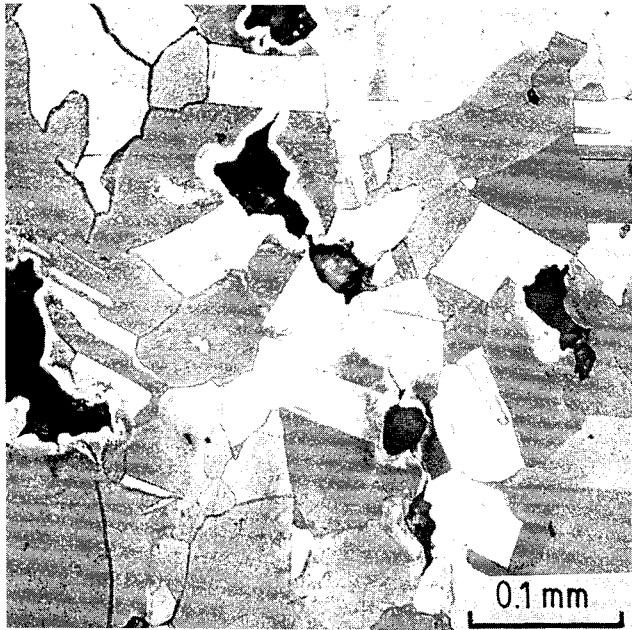
Fig. 13.

Specimen 411, 450°C, Cu-OFP, Etched. Little deformation within the grains, many large irregularly shaped cavities. No evidence of recrystallisation.
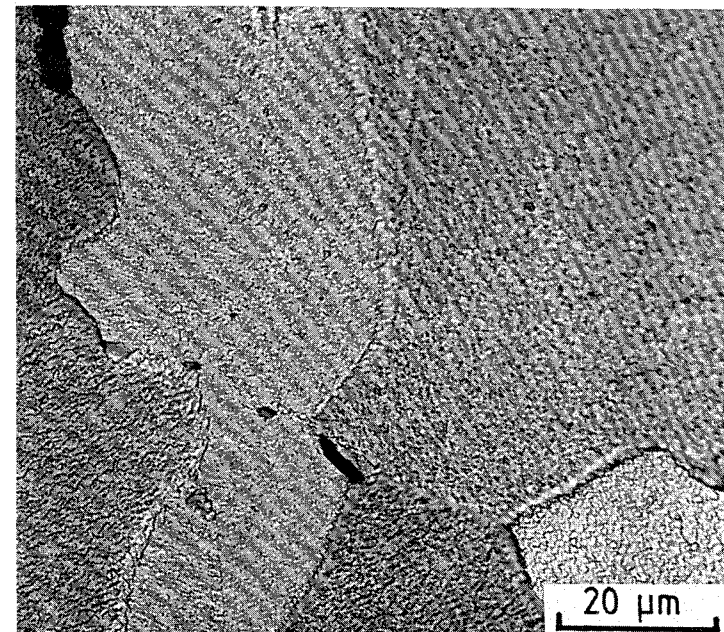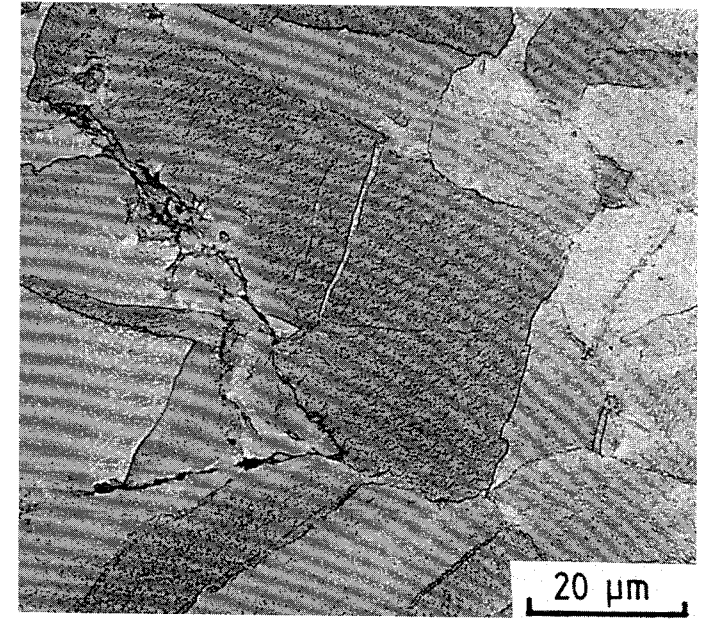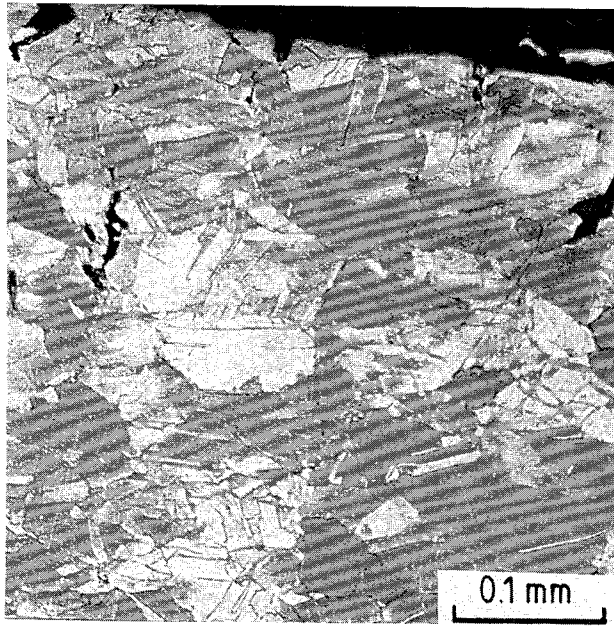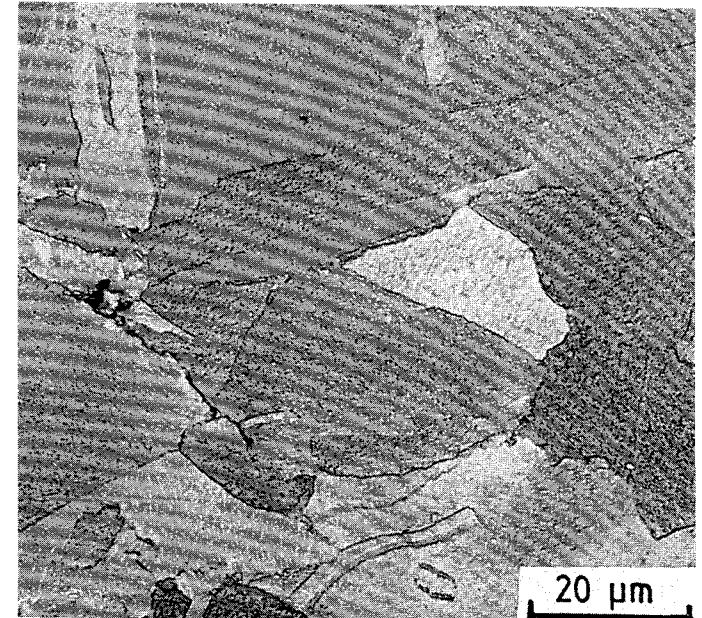
Fig. 14.

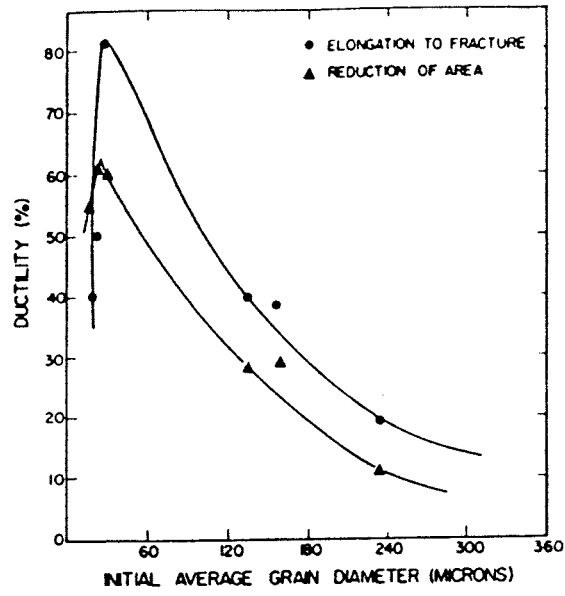Specimen 302, 215°C, Cu-OFS. Etched. Deformation within the grains cracks and cavities at grain boundaries.
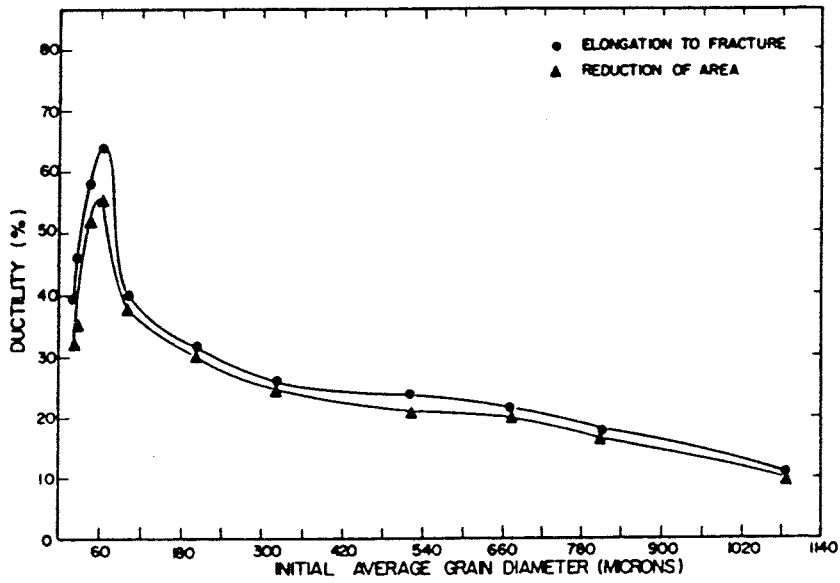

σ
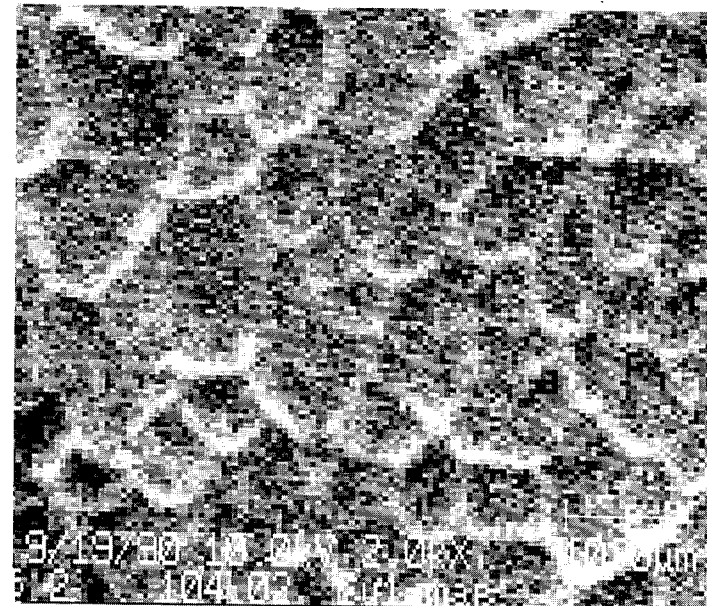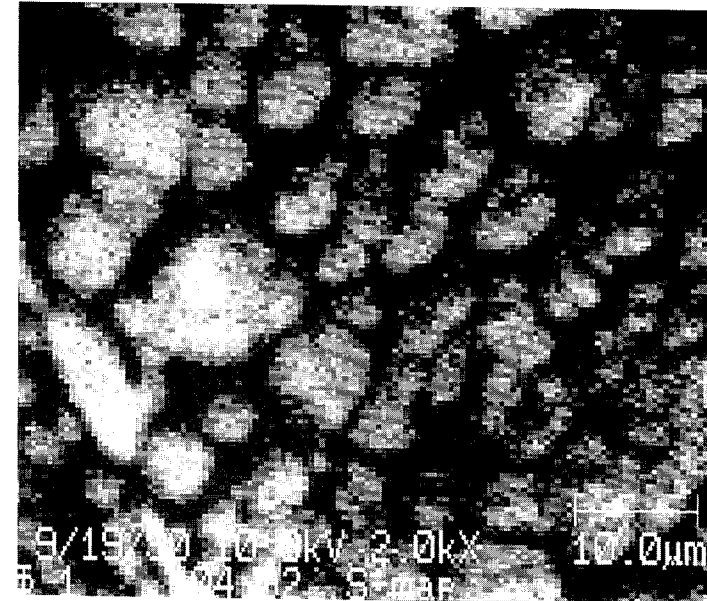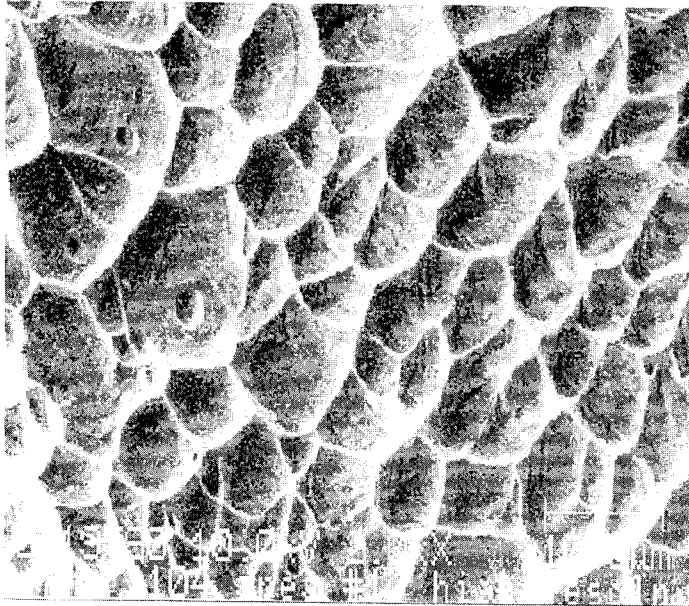
Fig. 15.

Scanning Auger Micrographs of a Fracture surface of specimen 104 (specimen fractured in microscope). Above right Sulphur map.
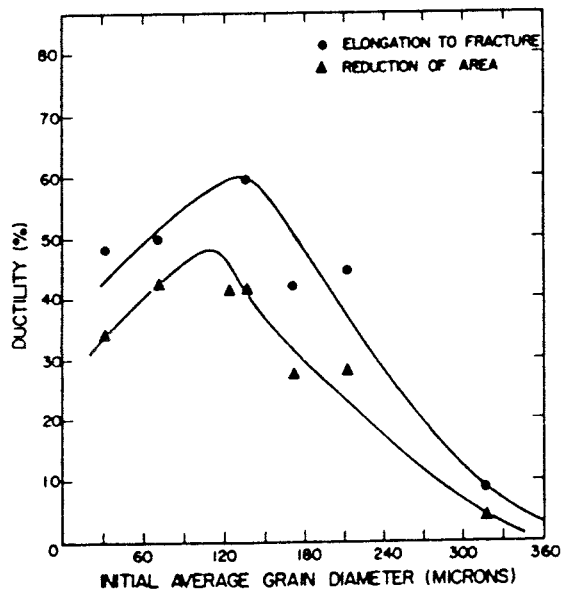Right Copper map.
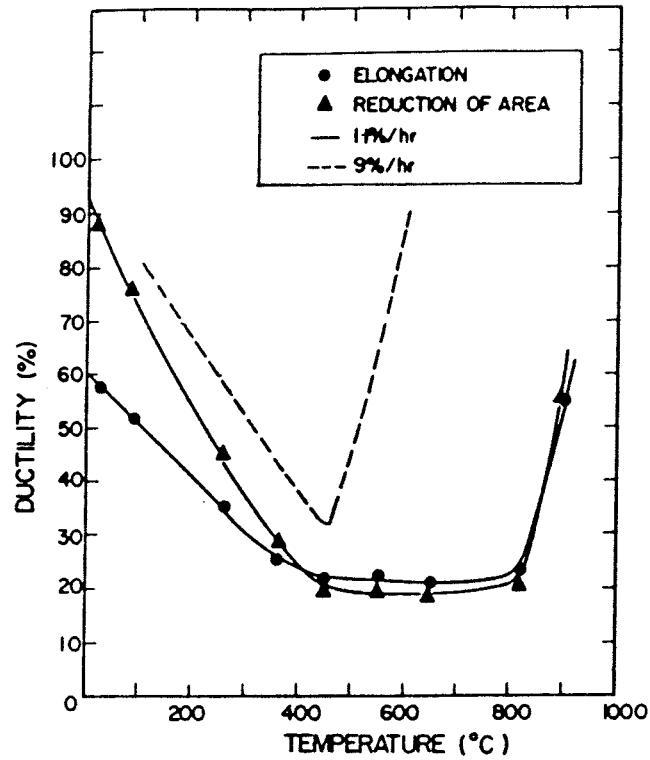Light areas indicate a high concentration of the elements.

—Effect of grain size on the ductility of copper at a
strain rate of 10^{-2} hr^{-1} and temperatures of (a) 350°C,
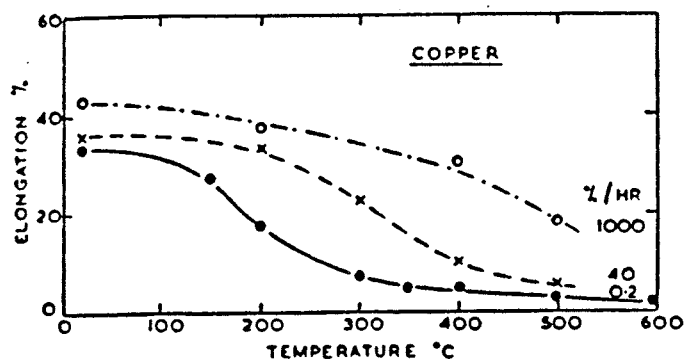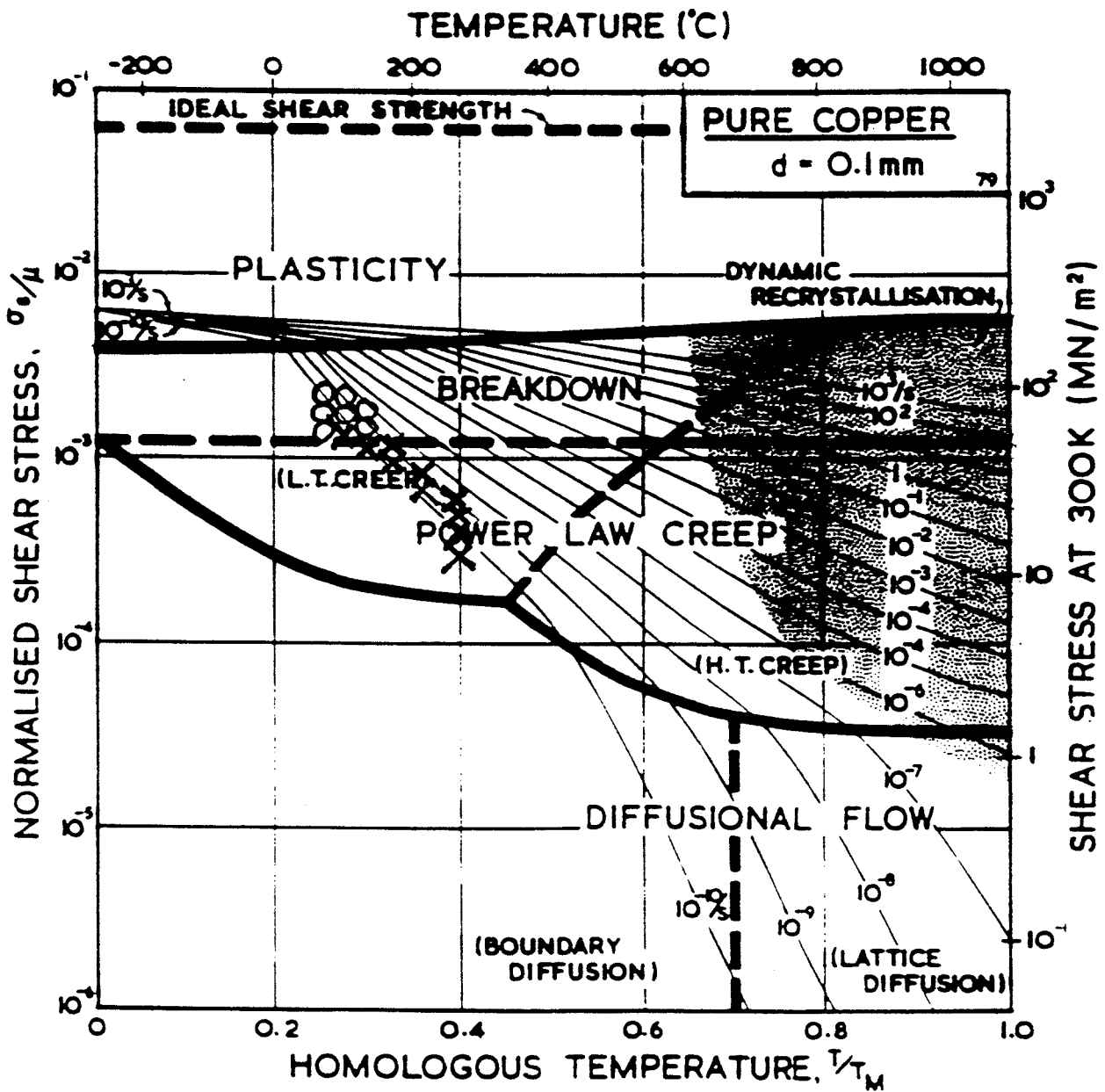(b) 425°C, and (c) 500°C.

Fig. 16.   From ref 10.

—Effect of test temperature on the ductility of copper
at strain rates of 10^{-2} and 10^{-1} hr^{-1}.

Fig. 17. From Ref 10. Grain size = 320 μm. Specimens 0.63 mm thick.

Influence of strain rate and temperature on the
ductility of copper.

Fig. 18. From Ref 11. Grain size = < 100 μm. Specimens 0.73 mm thick.

Pure copper with a grain size of 0·1 mm, including power-law breakdown.

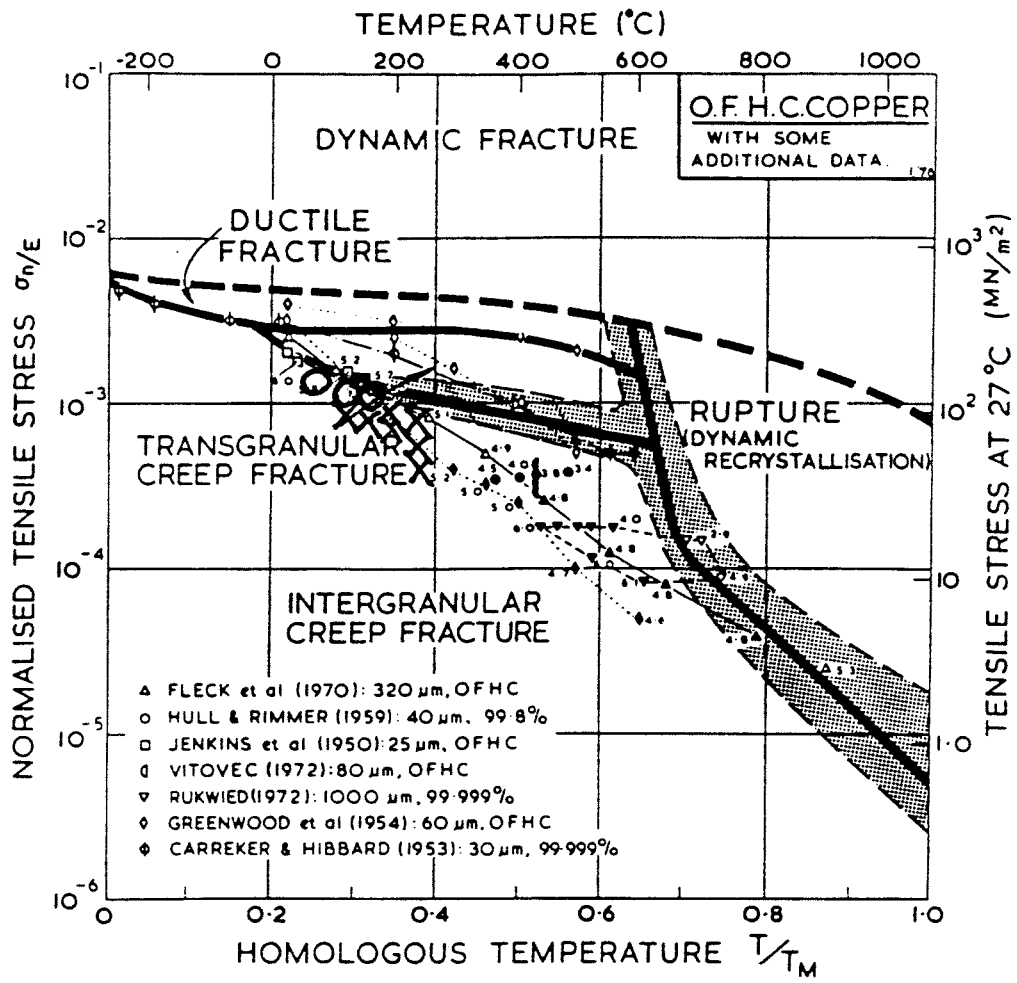Fig. 19   Deformation - mechanism map. From Ref. 12.O represents transgranular, X represents intergranular fracture.

Fig. 20   Fracture - mechanism map. From Ref. 13.

List of SKB reports

Annual Reports

1977-78
TR 121
KBS Technical Reports 1 – 120
Summaries
Stockholm, May 1979

1979
TR 79-28
The KBS Annual Report 1979
KBS Technical Reports 79-01 – 79-27
Summaries
Stockholm, March 1980

1980
TR 80-26
The KBS Annual Report 1980
KBS Technical Reports 80-01 – 80-25
Summaries
Stockholm, March 1981

1981
TR 81-17
The KBS Annual Report 1981
KBS Technical Reports 81-01 – 81-16
Summaries
Stockholm, April 1982

1982
TR 82-28
The KBS Annual Report 1982
KBS Technical Reports 82-01 – 82-27
Summaries
Stockholm, July 1983

1983
TR 83-77
The KBS Annual Report 1983
KBS Technical Reports 83-01 – 83-76
Summaries
Stockholm, June 1984

1984
TR 85-01
Annual Research and Development Report 1984
Including Summaries of Technical Reports Issued
during 1984. (Technical Reports 84-01 – 84-19)
Stockholm, June 1985

1985
TR 85-20
Annual Research and Development Report 1985
Including Summaries of Technical Reports Issued
during 1985. (Technical Reports 85-01 – 85-19)
Stockholm, May 1986

1986
TR 86-31
SKB Annual Report 1986
Including Summaries of Technical Reports Issued
during 1986
Stockholm, May 1987

1987
TR 87-33
SKB Annual Report 1987
Including Summaries of Technical Reports Issued
during 1987
Stockholm, May 1988

1988
TR 88-32
SKB Annual Report 1988
Including Summaries of Technical Reports Issued
during 1988
Stockholm, May 1989

1989
TR 89-40
SKB Annual Report 1989
Including Summaries of Technical Reports Issued
during 1989
Stockholm, May 1990

1990
TR 90-46
SKB Annual Report 1990
Including Summaries of Technical Reports Issued
during 1990
Stockholm, May 1991

1991
TR 91-64
SKB Annual Report 1991
Including Summaries of Technical Reports Issued
during 1991
Stockholm, April 1992

Technical Reports
List of SKB Technical Reports 1992

TR 92-01
GEOTAB. Overview
Ebbe Eriksson[1], Bertil Johansson[2], Margareta
Gerlach[3], Stefan Magnusson[2], Ann-Chatrin Nils-
son[4], Stefan Sehlstedt[3], Tomas Stark[1]
[1]SGAB, [2]ERGODATA AB, [3]MRM Konsult AB
[4]KTH
January 1992

TR 92-02
Sternö study site. Scope of activities and main results
Kaj Ahlbom[1], Jan-Erik Andersson[2], Rune Nordqvist[2], Christer Ljunggren[3], Sven Tirén[2], Clifford Voss[4]
[1]Conterra AB, [2]Geosigma AB, [3]Renco AB, [4]U.S. Geological Survey
January 1992

TR 92-03
Numerical groundwater flow calculations at the Finnsjön study site – extended regional area
Björn Lindbom, Anders Boghammar
Kemakta Consultants Co, Stockholm
March 1992